Separation and Purification Technology 177 (2017) 363–373

Contents lists available at ScienceDirect

Separation and Purification Technology

journal homepage: www.elsevier.com/locate/seppur

Electrocoagulation treatment of mine water from the deepest working European metal mine – Performance, isotherm and kinetic studies

Elham Nariyan [a,*], Mika Sillanpää [a,b], Christian Wolkersdorfer [a,c]

[a] Laboratory of Green Chemistry, Faculty of Technology, Lappeenranta University of Technology, Sammonkatu 12, 50130 Mikkeli, Finland
[b] Civil and Environmental Engineering, Florida International University, 10555 W. Flagler Street, EC 3680, Miami, FL 33174, United States
[c] SARChI Chair for Acid Mine Drainage Treatment, Tshwane University of Technology, Department of Environmental, Water and Earth Sciences, Private Bag X680, Pretoria 0001, South Africa

ARTICLE INFO

Article history:
Received 2 June 2016
Received in revised form 1 December 2016
Accepted 27 December 2016
Available online 5 January 2017

Keywords:
Electrocoagulation
Mine water
Isotherm
Kinetics

ABSTRACT

Electrocoagulation was investigated for the removal of copper, silicon, manganese, aluminum, iron and zinc as well as sulfate from real mine water. Batch experiments with monopolar iron anode and stainless steel cathode as well as monopolar aluminum anode and stainless steel cathode were conducted separately to identify the best electrocoagulation conditions. The removal efficiency in mine water increased with increasing reaction time and increasing current density and the type of electrodes affected the metals and sulfate removal as could be shown by the adsorption isotherms. Copper and silicon were obeying a Langmuir isotherm with an iron anode, whereas they were following a Freundlich isotherm when an aluminum anode was applied. The aluminum electrode resulted in a higher Langmuir constant q_{max} for all metals, while the iron electrode showed a better efficiency for removing the metals. This might be a result of the higher kinetic rate of iron compared to aluminum. Sulfate removal was better with aluminum electrodes resulting in removal rates of up to 41%, removing up to 5700 mg/L sulfate from the initial sulfate concentrations, whereas iron could only remove 3833 mg/L of sulfate from the real mine water. Furthermore, sulfate removal by aluminum electrode was faster compared to iron electrode.

1. Introduction

Metals discharging into water are considered a major problem for the smelting, electroplating and mining industries. For example, zinc, manganese and copper are considered toxic at elevated concentrations [1–3]. Silica in the form of silicic acid in mine water can produce severe scaling problems [4]. The most important parameters which can influence metal removal are redox potential (E_h) and pH [5,6]. Increasing the pH value is usually the most relevant removal step in metal laden waters, as this causes most metals to precipitate [7]. Different methods have been used for metal removal including chemical precipitation, biosorption, coagulation/flocculation, membrane filtration, biological, ion exchange, ozone oxidation and electrocoagulation [1,3,8,9]. Another highlighted environmental problem in mines are high concentrations of sulfate, which can reach up to several thousand milligrams per liter [10] and might severely affect receiving water courses, as it is usually connected to acid mine drainage. Discharge limits for sulfate are getting more restricted [11], as sulfate in water can deduce its taste and might cause health problems at high concentrations [12]. Current methods for removing sulfate are precipitating with lime [10], reverse osmosis, electrodialysis, adsorption [12], ion exchange [13] and electrocoagulation [14]. Electrocoagulation involves applying electricity to the electrodes for removing contaminants and it is used for treating water that, among others, contains COD, oil wastes or metals [1].

Removing metals from mine water with electrocoagulation is promising as it would generate sludge in the pH range of 6–7 and metal oxides which will not be discharged into receiving water courses [15,16]. In the electrocoagulation process, the pH of the solution will be adjusted to neutral during the reaction time, which is one of the benefits of this method. The pH near the cathode is alkaline as hydrogen is released and near the anode it is acidic as H^+ is produced [17]. Other benefits of using electrocoagulation are that it is easy to operate, it produces treated water with a high quality and it is already implemented as an effective method for precipitating contaminants [8]. Furthermore, electrocoagulation can produce more compact sludge compared to conventional coagulation [18]. Electrocoagulation can be summarized as consisting

* Corresponding author.
E-mail addresses: nariyanelham@gmail.com (E. Nariyan), Mika.Sillanpaa@lut.fi, Mika.sillanpaa@fiu.edu (M. Sillanpää), christian@wolkersdorfer.info (C. Wolkersdorfer).

http://dx.doi.org/10.1016/j.seppur.2016.12.042
1383-5866/

of the following processes (Fig. 1): (1) corroding of the anode and producing coagulant particles, (2) contaminants are destabilized and (3) eventually agglomeration of the destabilized phases produces flocs [18].

Different anodes can be used for the electrocoagulation process: magnesium, barium, zinc, chromium, calcium, silicon, cadmium or sodium have already been studied as electrodes. However, iron and aluminum have the superiority of producing multivalent ions which favor the electrocoagulation processes [19,20]. Nowadays, iron or aluminum are mostly used as sacrificial electrodes in electrocoagulation [16,21,22]. These different anodes have also different capacities for removing metals. For example, arsenic can better be removed by iron than by aluminum electrodes because ferric oxides have a higher adsorption capacity than hydrous aluminum oxides for As(III) removal [21].

In the electrocoagulation process (Fig. 1), iron and aluminum are released in the forms of poly-oxyhydroxide complexes and oxides as coagulants [23,24] for which metals are competing to react with them [25]. Conversion of iron(II) to iron(III) enhances the efficiency of electrocoagulation [26]. Ambulating aluminum atoms on the metal interface can be summarized as follows: Al^{+} is produced and will change to Al^{3+}; then Al^{3+} will be transferred by a diffusion mechanism which is affected by the concentration gradient and anions in the electrolyte [27]. The electrocoagulation process is influenced by various parameters such as the type of electrodes, time of reaction and the current density [28–30].

Passivation of the electrodes is one of the struggles which electrocoagulation is dealing with. For ameliorating this issue, there are suggestions such as using chloride anions [24,26,31], changing the polarity of the electrodes, optimization of the electrocoagulation reactor [26] and, finally, using sonication [32]. It is recommended to use stainless steel as a cathode when the water contains calcium and magnesium for avoiding anode passivation [16,17,27].

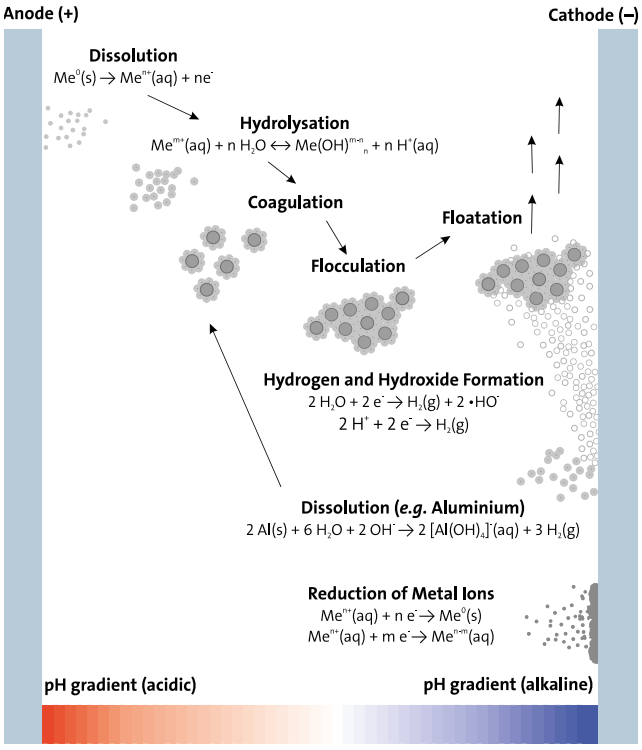

Fig. 1. Scheme of typical reactions encountered during electrocoagulation (modified after [18]).

In order to optimize the electrocoagulation process, different experiments were conducted in this study to identify the optimal current density, time and kind of electrode for removing metals and sulfate. Current density will define the amount of coagulant released into the water (Fe^{2+} or Al^{3+}). Thus, the current density will have an effect on the increasing of the flocs [33], and with increasing time, the removal efficiency will increase, too [34]. Moreover, with increasing time, the amount of released aluminum or iron from the sacrificial electrodes will increase in the solution and therefore, augmentation in coagulation and complexation will occur [8,35]. Also, the hydroxide concentration will be enhanced, which will result in a higher efficiency in metal precipitation as hydroxides [35]. Electrocoagulation can be used for removing metals and sulfate. In the electrocoagulation process, sulfate is considered to be adsorbed on metal hydroxide/oxides [36,37] and removing sulfate at lower pH ranges has a better efficiency than at higher pH values. Using aluminum and iron electrodes, sulfate removal by electrocoagulation is influenced by physical interactions with coagulants [36]. In electrocoagulation, metal removal can be affected by the affinity between the metals and the coagulant and their initial concentration [38]. Sulfate is getting a major problem in mining and mining companies are struggling to deal with the high concentration of sulfate. So far, the removal of metals and especially sulfate from real mine water by electrocoagulation was not studied in much detail.

The purpose of the present work is to assess electrocoagulation for removing aluminum, iron, manganese, copper, zinc, silicon and sulfate from real mine water of the Pyhäsalmi Mine, Finland by aluminum and iron electrodes in a batch system. It should be shown to which degree the metals and sulfate can be removed simultaneously. The Pyhäsalmi mine is 1444 m deep, making it currently the deepest base metal underground mine in Europe [39]. Metal and sulfate removal was varied depending on the electrode used. Specifically, the effect of current density, time and various electrodes on removing aluminum, iron, manganese, copper, zinc, silicon and sulfate from real mine water were studied. As sulfate removal by electrocoagulation was little investigated so far, this paper will identify possibilities of sulfate removal from real mine water as an alternative method to existing processes.

2. Materials and methods

2.1. Experimental procedure

Both aluminum and iron were used as sacrificial electrodes and stainless steel was used as the cathode in a monopolar configuration with plates having dimensions of 70 × 50 mm. Before each experiment, the electrodes were washed in 0.2 M HCl and thereafter rubbed with sand filter paper. Direct current (DC) power supply (GW INSTEK psp-405) with a voltage and an electrical current range of 0–40 V and 0–5 A was connected to the electrodes. In the experiments, the solutions were stirred constantly with a magnetic stirrer and a rotational speed of 200 rpm (rotations per minute). Furthermore, the distance between the electrodes was set to 0.5 cm to decrease the IR-drop [28].

The water was collected from the +500 m level in the Pyhäsalmi mine and stored in a cold room at −20 °C. A filtered aliquot was used and its chemical water quality parameters are given in Table 1.

All beakers were filled with 500 mL of mine water while the DC supply was adjusted to give the desired current. The samples were filtered with a 25 mm syringe filter (0.2 μm cellulose acetate membrane) for ICP-OES analysis. Both, pH and redox potential were measured with an intelliCAL™ pHC101 pH probe and intelliCAL™ MTC101 redox probe connected to a Hach HQ40d. The pH elec-

Table 1
Analysis of mine water obtained from the Pyhäsalmi Mine, Oulu Province, Finland (sampling date 2015–01–12). Calculation of TDS based on site specific EC to TDS ratio of 1.86. Charge balance error: −1.47.

Parameter	Unit	Value	Moles
pH (field)	–	2.68	2.089×10^{-3}
Cd	mg/L	2.1	1.901×10^{-5}
U	mg/L	0.620	0.270×10^{-3}
Zn	mg/L	960	1.494×10^{-2}
Si	mg/L	33	5.588×10^{-4}
Cu	mg/L	88	1.409×10^{-3}
Mn	mg/L	49	9.075×10^{-4}
Ca	mg/L	290	7.362×10^{-3}
Mg	mg/L	1200	5.022×10^{-2}
Fe	mg/L	770	1.403×10^{-2}
Al	mg/L	700	2.640×10^{-2}
As	mg/L	0.023	3.124×10^{-7}
SO_4^{2-}	mg/L	13000	1.377×10^{-1}
Electrical conductivity κ (field)	µS/cm	10657	–
Redox (field, corrected)	mV	467	–
Temperature (field)	°C	16.70	–
Color (laboratory)	–	Yellow-brownish	–
TDS (calculated)	mg/L	19790	–

trode was calibrated according to the operating manual. Metals were measured by ICP-OES (iCAP 6300, Thermo Electron Corporation) and sulfate was measured by a discrete analyzer (Ramboll Analytics method RA2087). All experiments were conducted at ambient temperature.

The removal efficiency is defined as follows:

$$\text{Removal efficiency, } \% = \frac{(C_0 - C_t)}{C_0} \times 100 \quad (1)$$

where C_0 and C_t are concentrations at time 0 and t, respectively.

Water analyzes were interpreted with PHREEQC 3.2 (WATEQ4F database) to determine the different species in the mine water with their molarities and the controlling phases for the mine water chemistry (Table 2). It is noteworthy to indicate that mine water has a complicated matrix which could burden changes during time.

3. Result and discussion

3.1. Effect of current density and time on metal removal by iron-stainless steel electrodes

The current density effect was investigated in various current density ranges of 10, 40 and 70 mA/cm^2 with an electrode pair of iron–stainless steel anode/cathodes. These current densities were chosen as they might be considered possible in a real mine water treatment plant, where an excess use of energy might be indisputable. It could be shown that increasing current densities increases the metal removal rates (Fig. 2). When iron stainless steel electrodes were utilized, 21.7, 65.5 and 100% aluminum removal was achieved after 60 min of electrocoagulation at current densities of 10, 40, 70 mA/cm^2, respectively. Moreover, with passing time, the removal efficiency increased, too. The increasing of removal efficiency with increasing reaction time and increasing current density is based on Faraday's law. Increasing reaction time and time would result in more Fe^{3+} species releasing in water as coagulant [40]. Copper had a removal efficiency of 41.9, 57.2 and 100% at current densities of 10, 40 and 70 mA/cm^2 after 60 min reaction time. Subsequently, silicon had a removal efficiency of 19.7, 42.8 and 87.7% at current densities of 10, 40 and 70 mA/cm^2, while zinc showed a removal efficiency of 15.6, 1.4 and 78.2% at 10, 40 and 70 mA/cm^2 after 120 min experimental time. As manganese removal in the form of $Mn(OH)_2$ will only be achieved above a pH 10 [41], there was a very small amount of manganese removed since the pH of the mine water did not increase that high. Manganese removal after 60 min was 10.7, 5.8 and 23.4% with 10, 40 and 70 mA/cm^2 current density. Finally, in regards to sulfate removal, there was no removal during the first 60 min of the reaction at current densities of 10 and 40 mA/cm^2. Yet, a removal rate of 7.9% was achieved with 70 mA/cm^2 after 60 min of electrocoagulation. Rising the current density from 10 to 70 mA/cm^2 resulted in an enhanced metal and sulfate removal with an aluminum, copper, silicon, zinc, manganese and sulfate removal of 40.5, 65.7, 33.6, 24.5, 12.5 and 0% to 100, 99.8, 89.2, 97.5, 26.9 and 28.9% (Fig. 2a–f). Specifically, the iron electrode removed 3500 mg/L of sulfate in the solution at optimal working conditions.

3.2. Effect of current density and time on metal removal by aluminum stainless steel electrodes

As could be shown, with increasing current density, the efficiency of the metal removal with aluminum–stainless steel anode/cathode electrodes increases, too (Fig. 3). Explicitly, with aluminum–stainless steel electrodes, iron was removed at 28.2, 51 and 67.9% after 60 min and current densities of 10, 40, 70 mA/cm^2, respectively.

Iron removal could be enhanced by increasing the time and current density. The improving iron removal can be attributed to an increase of soluble aluminum hydroxide acting as a coagulant [42]. Furthermore, with increasing time, the removal efficiency increases too. During 60 min coagulation time, pollutants removal rates reached to their maximum amount in the 70 mA/cm^2 current density. The highest removal is attributed to the silicon and iron, whereas the lowest is for manganese, sulfate and zinc. Manganese removal was neglectable with an aluminum–stainless steel anode/cathode configuration. This can be explained by the pH value of the solution being below 10, which would be the minimum pH needed for sustainable manganese precipitation [41,43]. Sulfate removal was not achieved at low current densities, but increased to 13.9% at 70 mA/cm^2 and 60 min reaction time. Increasing the current density from 10 to 70 mA/cm^2 results in an improvement in the removal efficiencies of metals and sulfate. Specifically, iron was removed 48.6% at a current density of 10 mA/cm^2, whereas its removal increased to 74.7% at a current density of 70 mA/cm^2. This trend is the same for other metals and sulfate (Fig. 3a–f).

3.3. Effect of electrode material on the metal removal

The electrode material has a substantial effect on the electrocoagulation process, as has been observed by various studies [24]. Based on the results presented here, the metal removal with iron electrodes is higher compared to that of aluminum electrodes (Figs. 2 and 3). Zinc removal is much higher with iron electrodes (97.5%) compared to an aluminum electrode, which is 37.6% after 120 min of electrocoagulation. Copper and manganese removal are also slightly higher by using iron compared to aluminum electrodes. This can be explained such that the aluminum electrodes release smaller particles than iron and consequently the efficiency of the iron electrode for metal removal will be higher than aluminum [16]. Furthermore, from the E_h-pH diagram, it becomes obvious why the removal efficiency of metals is higher with iron electrodes than aluminum electrodes (Fig. 4). Specifically, in various current densities, the iron electrodes increase the pH and decrease the E_h more than the aluminum electrodes, explaining why the metal removal with an iron electrode is higher compared to an aluminum electrode. The experiments also showed that the pH increase as well as the E_h decrease, and consequently the

Table 2
Summary of the controlling phases and relevant species resulting from the PHREEQC calculation.

Species	Molality	%	Controlling phases	Formula of controlling phases
$AlSO_4^+$	1.584×10^{-2}	60	Quartz	SiO_2
$Al(SO_4)_2^-$	7.279×10^{-3}	28	Jurbanite	$AlOHSO_4$
Al^{3+}	2.187×10^{-3}	8	Cristobalite	SiO_2
H_3AsO_3	5.146×10^{-16}	100	Chalcedony	SiO_2
$H_2AsO_4^-$	2.476×10^{-7}	79	Barite	$BaSO_4$
H_3AsO_4	6.471×10^{-8}	21	Maghemite	Fe_2O_3
$BaSO_4$	8.538×10^{-8}	68	Silica gel	SiO_2
Ba^{2+}	4.056×10^{-8}	32	Gypsum	$CaSO_4{\cdot}2H_2O$
Ca^{2+}	4.027×10^{-3}	55	Jarosite-Na	$NaFe_3(SO_4)2(OH)_6$
$CaSO_4$	3.285×10^{-3}	45	Anhydrite	$CaSO_4$
$CdSO_4$	7.706×10^{-6}	41	JarositeH	$(H_3O)Fe_3(SO_4)2(OH)_6$
Cd^{2+}	6.422×10^{-6}	34	$SiO_2(a)$	SiO_2
$Cd(SO_4)_2^{2-}$	4.813×10^{-6}	25		
Cl^-	3.989×10^{-4}	99		
Cu^+	5.269×10^{-13}	98		
Cu^{2+}	7.531×10^{-4}	53		
$CuSO_4$	6.558×10^{-4}	47		
AlF^{2+}	1.060×10^{-3}	94		
Fe^{2+}	4.856×10^{-3}	60		
$FeSO_4$	3.214×10^{-3}	39		
$FeSO_4^+$	4.165×10^{-3}	71		
$Fe(SO_4)_2^-$	1.314×10^{-3}	22		
Fe^{3+}	1.885×10^{-4}	3		
K^+	1.129×10^{-4}	92		
KSO_4^-	9.360×10^{-6}	8		
Mg^{2+}	2.730×10^{-2}	54		
$MgSO_4$	2.293×10^{-2}	46		
Mn^{2+}	5.491×10^{-4}	61		
$MnSO_4$	3.581×10^{-4}	39		
Mn^{3+}	2.217×10^{-18}	100		
NO_3^-	1.816×10^{-5}	100		
Na^+	1.776×10^{-3}	93		
$NaSO_4^-$	1.267×10^{-4}	7		
Ni^{2+}	2.034×10^{-5}	56		
$NiSO_4$	1.600×10^{-5}	44		
$PbSO_4$	2.932×10^{-8}	60		
Pb^{2+}	1.162×10^{-8}	24		
$Pb(SO_4)_2^{2-}$	8.126×10^{-9}	17		
SO_4^{2-}	5.464×10^{-2}	40		
$MgSO_4$	2.293×10^{-2}	17		
$AlSO_4^+$	1.584×10^{-2}	12		
$Al(SO_4)_2^-$	7.279×10^{-3}	5		
$ZnSO_4$	6.019×10^{-3}	4		
$FeSO_4^+$	4.165×10^{-3}	3		
$HSeO_3^-$	3.311×10^{-8}	55		
H_2SeO_3	2.745×10^{-8}	45		
SeO_4^{2-}	1.537×10^{-15}	97		
H_4SiO_4	5.588×10^{-4}	100		
$U(SO_4)_2$	1.068×10^{-24}	96		
USO_4^{2+}	4.330×10^{-26}	4		
UO_2^+	1.828×10^{-17}	100		
UO_2SO_4	1.637×10^{-6}	62		
$UO_2(SO_4)_2^{2-}$	6.516×10^{-7}	25		
UO_2^{2+}	3.591×10^{-7}	14		
Zn^{2+}	6.080×10^{-3}	41		
$ZnSO_4$	6.019×10^{-3}	40		
$Zn(SO_4)_2^{2-}$	2.842×10^{-3}	19		

removal efficiency of metals increases with increasing current densities.

Yet, silicon removal is slightly higher when using an aluminum electrode compared to an iron electrode. It is noteworthy that sulfate removal is better with an aluminum electrode compared to an iron electrode. The aluminum electrode removed 40.5% sulfate after 120 min, whereas the iron electrode removed 28.9% sulfate after 120 min of reaction. No sulfate removal was achieved in the lower current densities of 10 and 40 mA/cm^2.

3.4. Electrode consumptions

Electrode consumption is one of the key factors in the electrocoagulation process [8]. The amount of dissolved metals can be calculated by Faraday's law (Eq. (2)) in which m is the quantity of dissolved metals from the electrode (g), I is the current density (A/cm^2), t the time (s), M_w is the molecular weight of the electrode (g/mol), n is the oxidation reaction number and F is 96,485 C/mol as Faraday's constant [8,18,24].

$$m = \frac{I \times t \times M_w}{n \times F} \quad (2)$$

3.5. Kinetics and isotherms

In order to understand the electrocoagulation mechanisms, kinetic and isotherm constants were calculated (Tables 3–6). During the study, the sample volume (500 mL) and temperature were kept constant, while current densities were modified in the batch

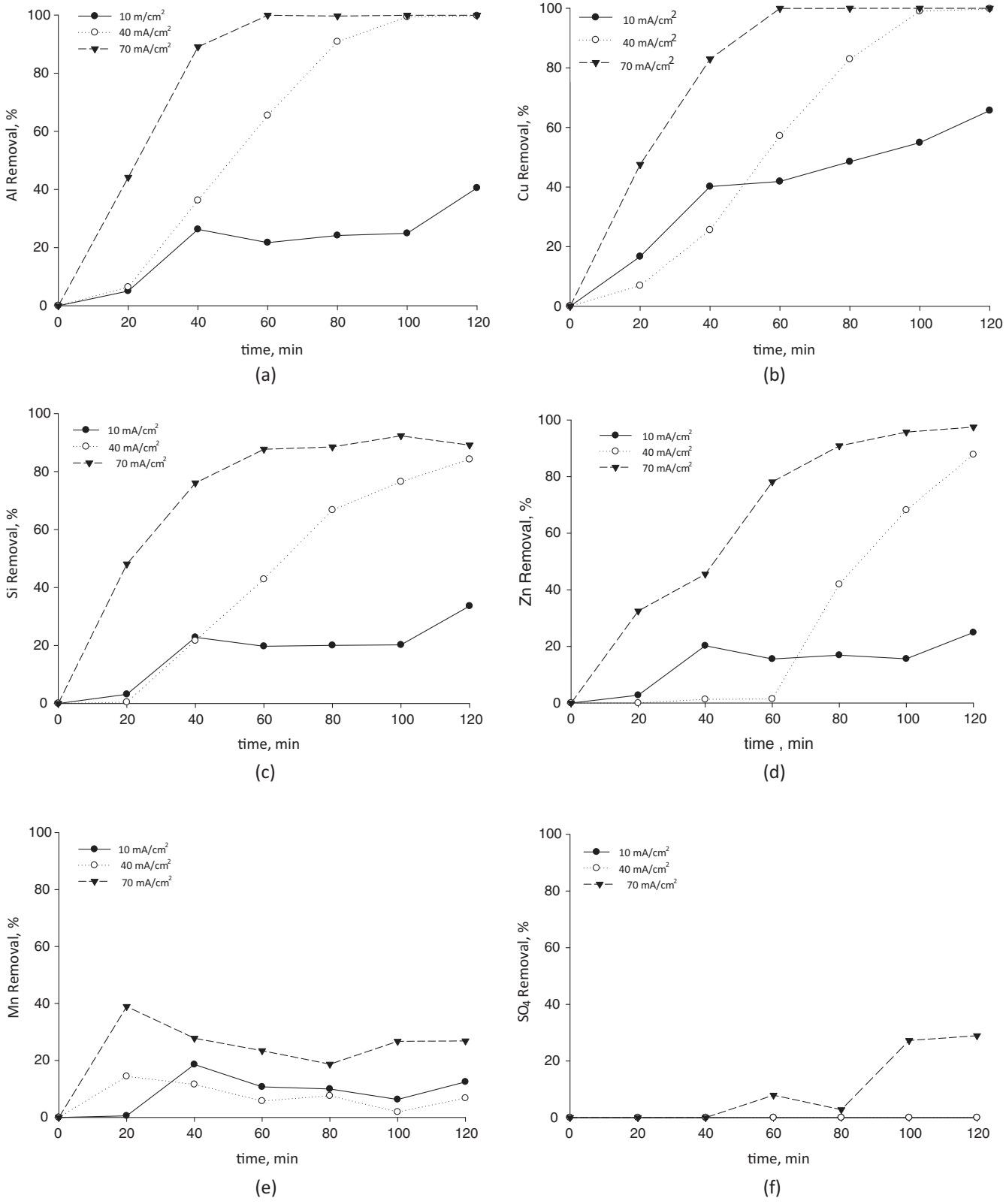

Fig. 2. Metal and sulfate removal efficiency at various current densities in electrocoagulation (iron–stainless steel anode/cathode configuration, pH: 2.68, κ: 10657 μS/cm) (a) Al; (b) Cu; (c) Si; (d) Zn;(e) Mn; (f) SO_4^{2-}.

system. The following Eqs. (3–5) for the first order, second order and pseudo first order kinetics were applied [8]:

$$C(t) = C_0 e^{-k_1 t} \quad (3)$$

$$\frac{1}{C(t)} = \frac{1}{C_0} + k_2 t \quad (4)$$

$$C(t) = C_e + (C_0 - C_e) e^{-k_{app} t} \quad (5)$$

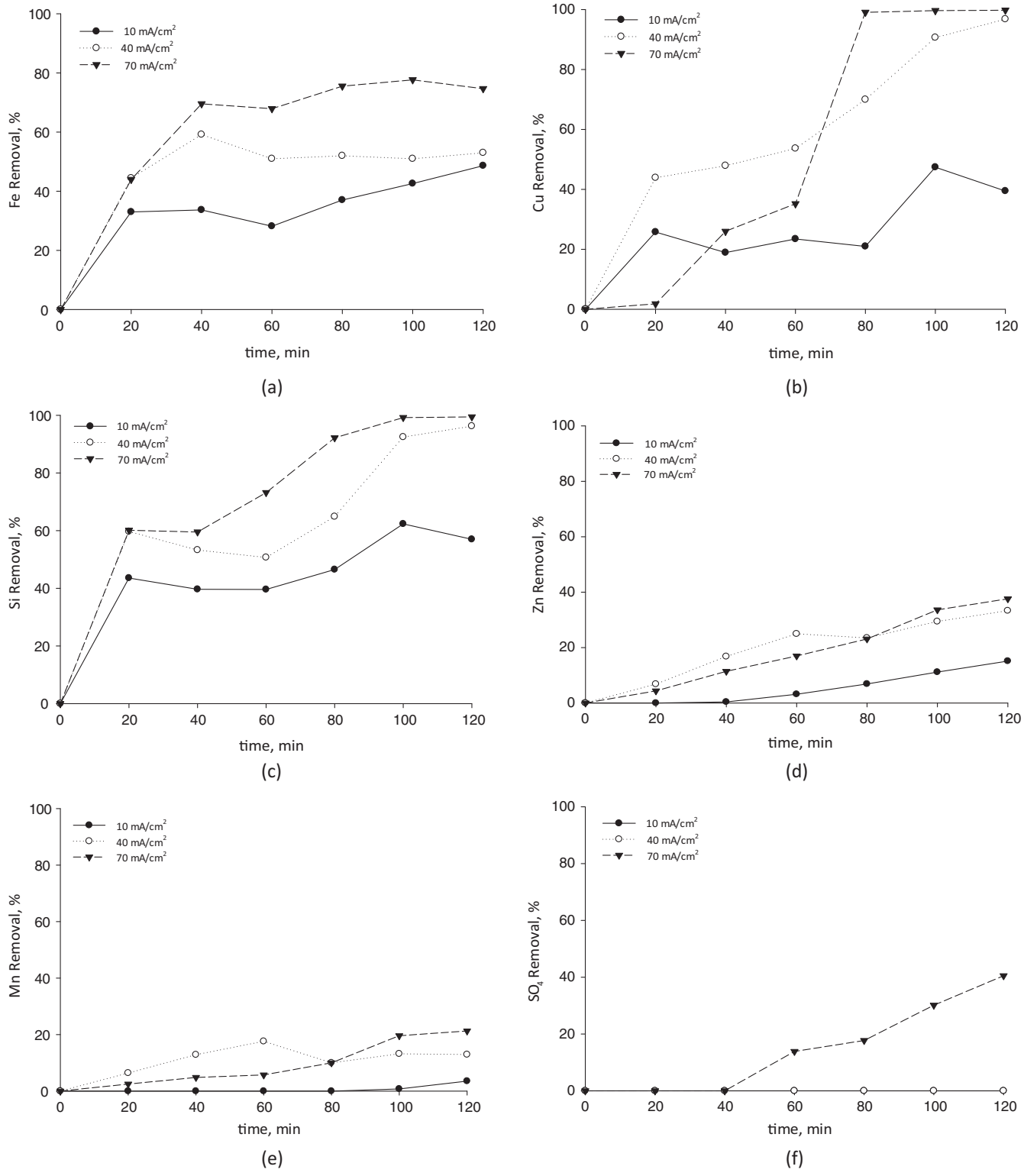

Fig. 3. Metal and sulfate removal efficiency at various current densities in electrocoagulation (aluminum–stainless steel anode/cathode configuration, pH: 2.68, κ: 10657 μS/cm) (a) Fe; (b) Cu; (c) Si; (d) Zn; (e) Mn; (f) SO_4^{2-}.

where k_1, k_2 and k_{app} are the first order, second order and pseudo first-order rate constants in min^{-1}, $(mg/L)^{-1}\,min^{-1}$ and min^{-1} [8].

As can be seen, for the iron anodes, copper, zinc and aluminum obey first order kinetics, suggesting that their adsorption is influenced by physical reactions [44]. Silicon obeys pseudo second orders kinetics, which indicates that the removal is affected by chemical reaction of Si^{4+} and the coagulant, specifically, by changing electrons [44]. k_1 and k_{app}, as expected, increase when the current density increases too [8]. The data shows that the rate of copper removal increased almost 1.5 times while the current density increased from 10 to 70 mA/cm^2 and the rate of aluminum removal increased 72 times when the current density increased

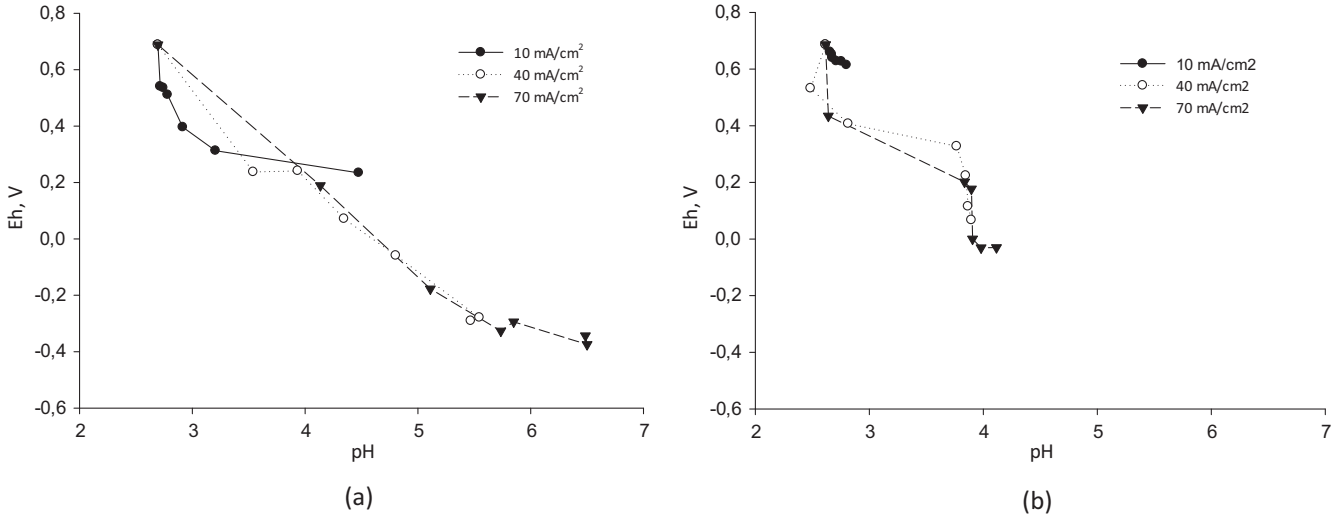

Fig. 4. E_h-pH diagram of (a) iron stainless steel electrodes and (b) aluminum stainless steel electrodes at various current densities during electrocoagulation.

Table 3
Calculated parameters for first-order, second order and pseudo second order removal rates of metal ions and sulfate at different current densities (CD) for iron–stainless steel anode/cathode combinations (solution volume: 500 mL, pH: 2.68 and κ: 10657 μS/cm) [8].

Parameter	CD (mA/cm^2)	First-order		Second order		Pseudo-second order	
		k_1 min^{-1}	R^2	k_2 (mg/L)$^{-1}$ × min^{-1}	R^2	k_{app} min^{-1}	R^2
Cu^{2+}	10	0.0089	0.8900	0.0004	0.9422	0.0173	0.9622
	40	0.0502	0.8808	0.0542	0.5795	0.0612	0.7255
	70	0.0134	0.9971	0.5201	0.5243	0.1101	0.6594
Si^{4+}	10	0.0010	0.4900	0.0002	0.4723	0.0026	0.7242
	40	0.0114	0.8834	0.0054	0.8487	0.0487	0.7910
	70	0.0139	0.6350	0.0056	0.5340	0.0239	0.9511
Zn^{2+}	10	0.0005	0.6522	2×10^{-6}	0.6574	0.0115	0.7680
	40	0.0102	0.6055	0.0001	0.5607	0.0179	0.6131
	70	0.0205	0.8788	0.0003	0.7414	0.0354	0.8369
Al^{3+}	10	0.0011	0.6674	9×10^{-5}	0.7665	0.0031	0.2515
	40	0.0422	0.8295	0.1189	0.6279	0.0121	0.2033
	70	0.0801	0.8320	1.9854	0.6850	0.0530	0.1421
Mn^{2+}	10	0.0013	0.0603	5×10^{-5}	0.1738	0.0155	0.3814
	40	0.0008		1×10^{-5}	0.0292	0.0041	
	70	0.0034		3×10^{-5}	0.0259	0.0201	0.2134
SO_4^{2-}	10	3×10^{-5}	0.0010	1×10^{-8}	0.0152	0.0027	0.0510
	40	0.0004	0.4367	3×10^{-8}	0.4294	0.0493	
	70	0.0024	0.6836	3×10^{-7}	0.7478	0.0082	0.1802

similarly. One of the possible explanations for this is the K_{sp} of aluminum hydroxide and copper hydroxide as it plays a key role in the removal efficiency [25]. While K_{sp} of $Cu(OH)_2$ is 2.2×10^{-20}, K_{sp} of $Al(OH)_3$ is 1.3×10^{-33} which might be one of the reasons, why k_1 for copper is considerably smaller than k_1 for aluminum, despite the fact that the initial concentration of aluminum was much higher than that for copper. Manganese obeys pseudo second orders kinetics and k_{app} increases with increasing current density. Sulfate obeys second order kinetic and it showed the same trend in increasing k_2 with increasing of current density. Manganese and sulfate show a small correlation coefficient (R^2) at low current densities which is due to a negligible removal rate.

Data for the first, second and pseudo-second order kinetic models for aluminum–stainless steel electrodes shows that copper, silicon and zinc obey a first order kinetic model (Table 4) and iron obeys pseudo-second order kinetics. Manganese and sulfate are following second order kinetics. As described above, all aforementioned metals that follow first order kinetics are adsorbed on the aluminum due to physical interaction [44]. Iron shows a different behavior and follows a pseudo second order kinetic model as it chemically adsorbs on the aluminum particles which are released from the anode [44].

It is noteworthy that both manganese and sulfate obey second order kinetics for aluminum anodes. Their kinetic rate (k_2) increases with increasing current density from 10 to 70 mA/cm^2. They show a small correlation coefficient (R^2) at low current densities which is due to a negligible removal rate.

The small removal rate for sulfate is due to its high initial concentration on one hand and the fact that non-optimal conditions for sulfate removal persisted during the experiments. Furthermore, as expected, k_1, k_2, and k_{app} are increasing with increasing current density. Zinc has a smaller k_1 than copper due to its initial concentration which is higher than copper. Specifically, the initial concentration of copper is 88 mg/L and zinc has the initial concentration of 960 mg/L. Furthermore, the k_{sp} of $Zn(OH)_2$ is higher than that of $Cu(OH)_2$ (1.2×10^{-17} *vs.* 2.2×10^{-20}) (Table 4).

Table 4
Calculated parameters for first-order, second order and pseudo second order removal rates of metal ions and sulfate at different current densities(CD) for aluminum–stainless steel anode/cathode combinations (solution volume: 500 mL, pH: 2.68 and κ: 10657 μS/cm) [8].

Parameter	CD (mA/cm^2)	First-order		Second order		Pseudo-second order	
		k_1 min^{-1}	R^2	k_2 (mg/L)$^{-1}$ × min^{-1}	R^2	k_{app} min^{-1}	R^2
Cu^{2+}	10	0.0040	0.5293	0.0003	0.5545	0.0093	0.2993
	40	0.0190	0.7797	0.0068	0.5588	0.0165	0.7725
	70	0.0465	0.7561	0.1003	0.5635	0.0142	0.7757
Si^{4+}	10	0.0036	0.1470	0.0014	0.1925	0.0047	0.2850
	40	0.0268	0.6636	0.1730	0.4904	0.0162	0.2351
	70	0.0280	0.7657	0.0290	0.7771	0.0016	0.1400
Zn^{2+}	10	0.0012	0.1570	10^{-6}	0.0129	0.0054	0.2475
	40	0.0036	0.9388	10^{-5}	0.9596	0.0117	0.1065
	70	0.0037	0.9669	2×10^{-5}	0.9589	0.0097	0.2128
Fe^{2+}	10	0.0038	0.4687	4×10^{-5}	0.5318	0.0229	0.4022
	40	0.0098	0.4702	0.0001	0.5944	0.0603	0.8597
	70	0.0057	0.5470	2×10^{-5}	0.0640	0.0321	0.6597
Mn^{2+}	10	0.0002	0.1300	-7×10^{-5}	0.1089	0.0011	0.1720
	40	0.0016	0.1581	6×10^{-5}	0.4152	0.0095	0.2050
	70	0.0018	0.8772	0.0001	0.8882	0.0092	0.1982
SO_4^{2-}	10	0.0002	0.0428	4×10^{-8}	0.0965	0.0330	0.0454
	40	0.0009	0.7286	8×10^{-8}	0.7395	0.0840	0.3333
	70	0.0034	0.7923	4×10^{-7}	0.8470	0.1402	0.5753

Table 5
Parameters and correlation coefficients for different adsorption isotherm models for metals and sulfate at various current densities of 10–70 mA/cm^2 for iron as anode and stainless steel as cathode.

Parameter	Langmuir isotherm			Freundlich isotherm			Dubinin-Radushkevich Isotherm		
	q_{max} (mg/g)	$1/q_{max}K_L$	R^2	ln(K_F)	b_F	R^2	$-B_DR^2T^2$	ln(q_D)	R^2
Cu^{2+}	10.41	0.0040	0.9999	1.6557	0.2012	0.6766	−0.3877	−0.1324	0.9972
Si^{4+}	1.3138	0.7045	0.9968	−0.4439	0.4132	0.9878	−0.7417	0.0536	0.9742
Zn^{2+}	48.309	0.1269	0.9993	3.2141	0.0979	0.9644	−18.891	3.7469	0.5256
Al^{3+}	10.82	0.0040	1.0000	2.0344	0.1122	0.9925	−0.0518	2.2974	0.9054
Mn^{2+}	0.174	−53.618	0.0098	9.9491	−3.7765	0.2386	581.84	−2.6973	0.2946
SO_4^{2-}	1428.57	18.516	0.0050	72.984	−7.3961	0.3618	4×10^8	0.4754	0.3435

Table 6
Parameters and correlation coefficients for different adsorption isotherm models for metals and sulfate at various current densities of 10–70 mA/cm^2 for aluminum as anode and stainless steel as cathode.

Parameter	Langmuir isotherm			Freundlich isotherm			Dubinin-Radushkevich Isotherm		
	q_{max} (mg/g)	$1/q_{max}K_L$	R^2	ln(K_F)	b_F	R^2	$-B_DR^2T^2$	ln(q_D)	R^2
Cu^{2+}	32.15	0.024	0.9881	2.602	0.391	0.9998	−0.1817	3.0255	0.8523
Si^{4+}	2.05	0.0221	0.9945	0.7525	0.3065	0.9999	−0.048	0.5255	0.9407
Zn^{2+}	0.723	−214.83	0.8349	120.82	−22.982	0.5878	300690	−7.5455	0.5580
Fe^{2+}	52.08	1.2763	0.0106	2.284	0.406	0.0081	270.04	3.8164	0.0020
Mn^{2+}	0.147	69.186	0.7145	20.841	−8.1718	0.9989	553.48	−3.0671	0.9975
SO_4^{2-}	909.09	14.133	0.9364	77.805	−7.7956	0.1159	4×10^8	1.9473	0.1159

3.6. Isotherms

Langmuir, Freundlich and the Dubininin-Radushkevich isotherms were applied to the experiments' results. The linear Langmuir isotherm is illustrated below (Eq. (6)) and models homogenous sorption [45]:

$$\frac{C_e}{q_e} = \frac{1}{K_L q_{max}} + \frac{C_e}{q_{max}} \tag{6}$$

q_{max} (mg/g) and K_L (L/mg) are the Langmuir constants, which are corresponding to the capacity of sorption and energy of adsorption, respectively. C_e (mg/L) and q_e (mg/g) are the equilibrium concentration and equilibrium adsorption capacity, respectively [45]. Metal adsorbed per gram of medium is q_t (mg/g), V is the solution volume (L), M is the electrode's dissolved weight (g), C_0 and C_t are the concentration of metal at any time t and the initial concentration (mg/L), respectively [46]. By plotting C_e/q_e *vs.* C_e, K_L and q_{max} can be extracted [45].

$$q_t = \frac{V(C_0 - C_t)}{M} \tag{7}$$

The Freundlich isotherm indicates one of heterogeneous adsorption, not monolayer and non-ideal adsorption (Eq. (8)) [45]:

$$\ln q_e = \ln K_F + b_F \ln C_e \tag{8}$$

where the concentration at equilibrium is defined by C_e (mg/L). b_F (dimensionless) and K_F (L/mg) are constants, which are influenced by the adsorption intensity and capacity, respectively [44,47–49].

Finally, the Dubinin-Radushkevich Isotherm is expressed as follows (Eq. (9)) [49]:

Table 7
Comparison of some removal efficiencies of metals and sulfate from industrial/synthetic water using electrocoagulation (–: not used in experiment).

Treatment method	Current or voltage	C_0 (mg/L)							R (%)							References
		Cu	Si	Fe	Al	Mn	Zn	SO_4	Cu	Si	Fe	Al	Mn	Zn	SO_4	
Electrocoagulation	4 mA/cm^2	45	–	–	–	–	–	–	100	–	–	–	–	–	–	[8]
6 Fe (carbon steel) electrodes	4 mA/cm^2	33.3	–	–	–	–	20.4	–	99	–	–	–	–	99		[8]
Iron stainless steel electrode	70 mA/cm^2	88	33	770	700	49	960	13000	100	89.17	–	99.96	26.85	97.52	28.89	This study
Aluminum stainless steel electrodes	70 mA/cm^2	88	33	770	700	49	960	13000	99.82	99.48	74.69	–	21.26	37.59	40.51	This study
Iron electrodes	3 A	18.71	–	–	–	–	8.20	–	78.57	–	–	–	–	75.48	–	[54]
Aluminum electrodes	3 A	18.71	–	–	–	–	8.20	–	48.08	–	–	–	–	98.71	–	[54]
2 Fe electrodes	0.04 A/cm^2	14.91	–	–	–	–	16.39	–	97	–	–	–	–	93	–	[55]
6 pairs of Al electrodes	30 A/m^2	50	–	–	13	6	–	–	99.9	–	–	95.6	84	–	–	[56]
Iron electrode	10 mA/cm^2	–	–	2.3	–	–	3.2	–	–	–	–	–	–	98.2	–	[35]
6 plate aluminum electrodes, monopolar, parallel	30 V	–	–	–	–	–	–	700	–	–	–	–	–	–	60	[57]
Iron as anode	62 mA/cm^2	–	–	–	–	–	–	500	–	–	–	–	–	–	30	[36]

$$q_e = q_D \exp\left(-B_D\left[RT\ln\left(1+\frac{1}{C_e}\right)\right]^2\right) \quad (9)$$

where q_D (mg/g) is the isotherm constant [50] and B_D (mol^2 J^{-2}) is the corresponding average free Energy sorption per mole of sorbate and can be calculated according to Eq. (10) [49,50]. In addition, T is the temperature (K) and R is the universal gas constant (8.314 J mol^{-1} K^{-1}) [50].

$$E = \frac{1}{\sqrt{2B_D}} \quad (10)$$

The Dubinin-Radushkevich isotherm constants can be obtained by a linear transformation of the x- and y-values to $(\ln(1 + 1/C_e))^2$ and $\ln(q_e)$, respectively. The slope is then $-B_D R^2 T^2$ and the intercept $\ln(q_D)$ [49]. As can be seen for the iron–stainless steel anode/cathode combination (Table 5), all of the pollutants except manganese and sulfate are obeying a Langmuir isotherm. Furthermore, it can be concluded from the Dubinin-Radushkevich isotherms that copper, silicon, zinc and aluminum have free sorption energies of 2.8, 2, 0.4 and 7.8 kJ/mol (the free energy can be calculated from Eq. (10)), which indicates that their removal is based on physical reactions [51], which is in good correlation with the aforementioned kinetic observations. As can be seen, the highest q_{max} is related to sulfate, as 3800 mg/L of its initial concentration was reduced by the iron–stainless steel anode/cathode, while manganese shows the smallest q_{max} as its removal was negligible.

As can be seen for aluminum–stainless steel electrodes (Table 6), zinc, iron and sulfate are obeying a Langmuir isotherm. However, copper, silicon and manganese obey a Freundlich isotherm.

In addition, using the Dubinin-Radushkevich isotherm, it can be deduced that copper and silicon have a mean free sorption energy of 4 and 7.9 kJ/mol respectively, which are indicative of physical adsorption [52,53]. These findings are also in good correlation with the kinetic studies. Finally, sulfate and manganese show the most and least q_{max}, due to the aforementioned reason for an iron–stainless steel anode/cathode combination, with a q_{max} of 909.1 and 2.55 mg/g, respectively. Due to the pH- and E_h-conditions of the experiments, manganese removal was negligible, as it is only removed at pH > ≈10 in most systems.

Metals and sulfate obey different isotherms with different anode material of iron and aluminum. Specifically, all of metals except manganese obey Langmuir isotherm, whereas this trend changed when aluminum anode was used. For instance, copper and silicon changed their adsorption from monolayer to non-monolayer and heterogeneous, when iron and aluminum anode were applied, respectively. Also, sulfate adsorption was changed when iron anode changed to aluminum anode. When iron was used the non-monolayer and heterogeneous adsorption was dominant, while it has changed to monolayer adsorption when aluminum anode was used.

Further research with real mine water needs to identify the mechanisms with which sulfate can be removed at much higher removal rates and interferences with the metals in solution could be suppressed. Different studies for metals and sulfate removal with electrocoagulation process have been done. Comparison of current study with other studies is shown (Table 7).

4. Conclusions

Electrocoagulation was found to be a prosperous technique for the removal of metals and sulfate in real mine water.

Removal efficiencies for various metals with different electrodes showed that metals are better removed by an iron electrode. The removal behavior of the metals can be explained by the E_h-pH and the metal's stability diagram. Yet, sulfate is better removed by an aluminum electrode.

The initial concentration seems to have a major effect on the removal rate and the kinetics of the reaction. As can be seen, zinc and copper have initial concentrations of 960 and 88 mg/L, respectively, and the rate of reaction for copper at the beginning (0–20 min, 70 mA/cm^2, iron–stainless steel and aluminum–stainless steel) is almost 2.5 times higher than that for zinc. However, the reduction of the redox potential with copper is higher than with zinc amounting to +0.337 and −0.763 V, respectively.

Based on the kinetic modeling, the aluminum electrode is more efficient for metal removal than the iron electrode. Both, the free sorption energy calculation from the Dubinin-Radushkevich Isotherm and the k-parameter for the kinetics show that copper and silicon are influenced by physical interaction for removing by two electrodes, while zinc is merely being influenced by physical interaction by the iron electrode in the electrocoagulation process. All of the contaminants, except manganese and sulfate, obey a Langmuir isotherm when an iron electrode is applied. However, when an aluminum anode was utilized, the metals prevail a different behavior compared to the iron electrodes. Specifically, silicon, copper and manganese were obeying a Freundlich isotherm, whereas zinc and sulfate were obeying a Langmuir isotherm. Sulfate was better removed by an aluminum electrode compared to the iron electrodes with a maximum removal rate of 28.9 and 40.5%, respectively.

Acknowledgement

We appreciate the financial assistance of the Finnish Funding Agency for Technology and Innovation (TEKES) for the Intelligent Mine Water Management (iMineWa) project. We also acknowledge Pyhäsalmi mine for providing access and water samples. Finally, we thank Dr. Varsha Srivastava for her earlier comments on this paper.

References

[1] E. Gatsios, J.N. Hahladakis, E. Gidarakos, Optimization of electrocoagulation (EC) process for the purification of a real industrial wastewater from toxic metals, J. Environ. Manage. 154 (2015) 117–127.
[2] M. Al-Shannag, Z. Al-Qodah, K. Bani-Melhem, M.R. Qtaishat, Heavy metal ions removal from metal plating wastewater using electrocoagulation: kinetic study and process performance, Chem. Eng. J. 260 (2015) 749–756.
[3] J. Lu, Y. Li, M. Yin, X. Ma, S. Lin, Removing heavy metal ions with continuous aluminum electrocoagulation: a study on back mixing and utilization rate of electro-generated Al ions, Chem. Eng. J. 267 (2015) 86–92.
[4] W. Den, C.-J. Wang, Removal of silica from brackish water by electrocoagulation pretreatment to prevent fouling of reverse osmosis membranes, Sep. Purif. Technol. 59 (2008) 318–325.
[5] W. Stumm, J.J. Morgan, Aquatic Chemistry – Chemical Equilibria and Rates in Natural Waters, third ed., Wiley & Sons, New York, 1996.
[6] C. Wolkersdorfer, Water Management at Abandoned Flooded Underground Mines – Fundamentals, Tracer Tests, Modelling, Water Treatment, Springer, Heidelberg, 2008.
[7] C. Wolkersdorfer, Grubenwasserreinigung – Verfahren und Vorgehensweisen, Tshwane University of Technology, Pretoria, 2013, p. 198.
[8] M. Al-Shannag, Z. Al-Qodah, K. Bani-Melhem, M.R. Qtaishat, M. Alkasrawi, Heavy metal ions removal from metal plating wastewater using electrocoagulation: kinetic study and process performance, Chem. Eng. J. 260 (2015) 749–756.
[9] S.H. Seo, B.W. Sung, G.J. Kim, K.H. Chu, C.Y. Um, S.L. Yun, Y.H. Ra, K.B. Ko, Removal of heavy metals in an abandoned mine drainage via ozone oxidation: a pilot-scale operation, Water Sci. Technol.: J. Int. Assoc. Water Pollut. Res. 62 (2010) 2115–2120.
[10] E.-T. Tolonen, J. Rämö, U. Lassi, The effect of magnesium on partial sulphate removal from mine water as gypsum, J. Environ. Manage. 159 (2015) 143–146.
[11] I. Ñancucheo, D. Barrie Johnson, Removal of sulfate from extremely acidic mine waters using low pH sulfidogenic bioreactors, Hydrometallurgy 150 (2014) 222–226.
[12] D. Guimarães, V.A. Leao, Batch and fixed-bed assessment of sulphate removal by the weak base ion exchange resin Amberlyst A21, J. Hazard. Mater. 280C (2014) 209–215.
[13] E. Iakovleva, E. Mäkilä, J. Salonen, M. Sitarz, M. Sillanpää, Industrial products and wastes as adsorbents for sulphate and chloride removal from synthetic alkaline solution and mine process water, Chem. Eng. J. 259 (2015) 364–371.
[14] V. Orescanin, R. Kollar, A combined CaO/electrochemical treatment of the acid mine drainage from the "Robule" lake, J. Environ. Sci. Health A: Toxic/Hazard. Substances Environ. Eng. 47 (2012) 1186–1191.
[15] S. Powell Water, Powell Electrocoagulation – Sustainable Technology for the Future, Powell Water Systems, Centennial, 2001.
[16] P. Holt, G. Barton, C. Mitchell, Electrocoagulation as a wastewater treatment, in: Proceedings, Third Annual Australian Environmental Engineering Research Event, Castlemaine, 1999.
[17] G. Chen, Electrochemical technologies in wastewater treatment, Sep. Purif. Technol. 38 (2004) 11–41.
[18] M. Vepsäläinen, Electrocoagulation in the treatment of industrial waters and wastewaters, VTT Sci. 12 (2012) 1–96.
[19] O. Sahu, M. Bidyut, P.K. Chaudhari, Treatment of wastewater by electrocoagulation: a review, Environ. Sci. Pollut. Res. Int. 21 (2014) 2397–2413.
[20] M. Mickley, Treatment of concentrate, in: U.S. Department of the Interior Bureau of Reclamation, Denver Federal Center May, Mickley & Associates, 2008.
[21] C. Barrera-Díaz, B. Bilyeu, G. Roa, L. Bernal-Martinez, Physicochemical aspects of electrocoagulation, Sep. Purif. Rev. 40 (2011) 1–24.
[22] D. Kumarasinghe, L. Pettigrew, L.D. Nghiem, Removal of heavy metals from mining impacted water by an electrocoagulation-ultrafiltration hybrid process, Desalin. Water. Treat. 11 (2012) 66–72.
[23] S.M. Adapureddy, S. Goel, Optimizing electrocoagulation of drinking water for turbidity removal in a batch reactor, Int. Proc. Chem. Biol. Environ. Eng. 30 (2012) 97–102.
[24] H. Liu, X. Zhao, J. Qu, Electrocoagulation in water treatment, in: C. Comninellis, G. Chen (Eds.), Electrochemistry for the Environment, Springer, New York, 2010, pp. 245–262.
[25] A. Shafaei, M. Rezaie, M. Nikazar, Evaluation of Mn^{2+} and Co^{2+} removal by electrocoagulation: a case study, Chem. Eng. Process.: Process Intensif. 50 (2011) 1115–1121.
[26] Y. Gendel, O. Lahav, A new approach to increasing the efficiency of low-pH Fe-electrocoagulation applications, J. Hazard. Mater. 183 (2010) 596–601.
[27] M. Bennajah, Traitement des rejets industriels liquide par electrocoagulation electroflotation en reacteur airlift, in: École doctorale: Mécanique, énergétique, génie civil, procédés, Ecole Supérieure de Technologie de Casablanca (Maroc), Décembre 2007, pp. 204.
[28] I. Heidmann, W. Calmano, Removal of Zn(II), Cu(II), Ni(II), Ag(I) and Cr(VI) present in aqueous solutions by aluminium electrocoagulation, J. Hazard. Mater. 152 (2008) 934–941.
[29] V. Keerthi, N. Balasubramanian, Removal of heavy metals by hybrid electrocoagulation and microfiltration processes, Environ. Technol. 34 (2013) 2897–2902.
[30] M.S. Oncel, A. Muhcu, E. Demirbas, M. Kobya, A comparative study of chemical precipitation and electrocoagulation for treatment of coal acid drainage wastewater, J. Environ. Chem. Eng. 1 (2013) 989–995.
[31] G. Mouedhen, M. Feki, P. Wery Mde, H.F. Ayedi, Behavior of aluminum electrodes in electrocoagulation process, J. Hazard. Mater. 150 (2008) 124–135.
[32] V.K. Kovatcheva, M.D. Parlapanski, Sono-electrocoagulation of iron hydroxides, Colloids Surf. A 149 (1999) 603–608.
[33] B. Al Aji, Y. Yavuz, A.S. Koparal, Electrocoagulation of heavy metals containing model wastewater using monopolar iron electrodes, Sep. Purif. Technol. 86 (2012) 248–254.
[34] J. Chu, X. Shi, Y. Du, F. Ma, Experimental study for treating electroplating wastewater containing Cr^{n+}, Cu^{2+} and Zn^{2+} by electrocoagulation, J. Jiangsu Univ. (Nat. Sci. Ed.) 32 (2011) 103–106.
[35] H.J. Mansoorian, A.H. Mahvi, A.J. Jafari, Removal of lead and zinc from battery industry wastewater using electrocoagulation process: influence of direct and alternating current by using iron and stainless steel rod electrodes, Sep. Purif. Technol. 135 (2014) 165–175.
[36] M. Murugananthan, G.B. Raju, S. Prabhakar, Removal of sulfide, sulfate and sulfite ions by electro coagulation, J. Hazard. Mater. 109 (2004) 37–44.
[37] S. Pulkka, M. Martikainen, A. Bhatnagar, M. Sillanpää, Electrochemical methods for the removal of anionic contaminants from water – a review, Sep. Purif. Technol. 132 (2014) 252–271.
[38] D. Patrick, M. Nathalie, M. Guy, B. Jean-François, Removal of Pb^{2+} and Zn^{2+} ions from acidic soil leachate: a comparative study between electrocoagulation, adsorption and chemical precipitation processes, Int. J. Environ. Waste Manage. 8 (2011).
[39] T. Mäki, M. Imaña, J. Kousa, J. Luukas, The Vihanti-Pyhäsalmi VMS Belt, in: W. D. Maier, R. Lahtinen, H. O'Brien (Eds.), Mineral Deposits of Finland, Elsevier, 2015, pp. 507–530.
[40] M. Alizadeh, E. Ghahramani, M. Zarrabi, S. Hashemi, Efficient de-colorization of methylene blue by electro-coagulation method: comparison of iron and aluminum electrode, Iran. J. Chem. Chem. Eng.-Int. English Ed. 34 (2015) 39–47.
[41] G.A. Sincero, A.P. Sincero, Removal of iron and manganese by chemical precipitation, in: Physical-Chemical Treatment of Water and Wastewater, CRC Press, 2002.
[42] S. Vasudevan, J. Jayaraj, J. Lakshmi, G. Sozhan, Removal of iron from drinking water by electrocoagulation: adsorption and kinetics studies, Korean J. Chem. Eng. 26 (2009) 1058–1064.
[43] K.K. Kefeni, T.M. Msagati, J.P. Maree, B.B. Mamba, Metals and sulphate removal from acid mine drainage in two steps via ferrite sludge and barium sulphate formation, Miner. Eng. 81 (2015) 79–87.
[44] A.-S.A. Bakr, Y.M. Moustafa, E.A. Motawea, M.M. Yehia, M.M.H. Khalil, Removal of ferrous ions from their aqueous solutions onto $NiFe_2O_4$–alginate composite beads, J. Environ. Chem. Eng. 3 (2015) 1486–1496.
[45] V. de Oliveira Sousa Neto, G.S.C. Raulino, P.T.C. Freire, M.A. Araújo-Silva, R.F. do Nascimento, Equilibrium and kinetic studies in adsorption of toxic metal ions for wastewater treatment, in: A Book on Ion Exchange, Adsorption and Solvent Extraction, 2013, pp. 145–182.
[46] Y.A. Ouaissa, M. Chabani, A. Amrane, A. Bensmaili, Removal of tetracycline by electrocoagulation: kinetic and isotherm modeling through adsorption, J. Environ. Chem. Eng. 2 (2014) 177–184.
[47] E.H. Ezechi, S.R.b.M. Kutty, A. Malakahmad, M.H. Isa, Characterization and optimization of effluent dye removal using a new low cost adsorbent: equilibrium, kinetics and thermodynamic study, Process Saf. Environ. 98 (2015) 16–32.
[48] R. Kamaraj, P. Ganesan, S. Vasudevan, Removal of lead from aqueous solutions by electrocoagulation: isotherm, kinetics and thermodynamic studies, Int. J. Environ. Sci. Technol. 12 (2015) 683–692.
[49] Y.S. Ho, J.F. Porter, G. McKay, Equilibrium isotherm studies for the sorption of divalent metal ions onto peat: copper, nickel and lead single component systems, Water Air Soil Pollut. 141 (2002) 1–33.
[50] M. Irani, M. Amjadi, M.A. Mousavian, Comparative study of lead sorption onto natural perlite, dolomite and diatomite, Chem. Eng. J. 178 (2011) 317–323.
[51] M.A. Barakat, R. Kumar, Synthesis and characterization of porous magnetic silica composite for the removal of heavy metals from aqueous solution, J. Ind. Eng. Chem. 23 (2015) 93–99.
[52] A.U. Itodo, H.U. Itodo, Sorption energies estimation using Dubinin-Radushkevich and Temkin adsorption isotherms, Life Sci. J. 7 (2010).
[53] H.v. Philipsborn, Tafeln zum Bestimmen der Minerale nach äußeren Kennzeichen, second ed., Schweizerbart, Stuttgart, 1967.
[54] A.K. Yadav, L. Singh, A. Mohanty, S. Satya, T.R. Sreekrishnan, Removal of various pollutants from wastewater by electrocoagulation using iron and aluminium electrode, Desalin. Water Treat. 46 (2012) 352–358.

[55] V.K. Ninova, Electrochemical treatment of mine wastewaters containing heavy metal ions, in: Annual Mining and Mineral Processing (Part II), Sofia, 2003, pp. 215–220.
[56] J. Rodriguez, S. Stopic, B. Friedrich, Continuous electrocoagulation treatment of wastewater from copper production, World Metall. – Erzmetall 60 (2007) 81–87.
[57] A.H. Mahvi, H.J. Mansoorian, A. Rajabizadeh, Performance evaluation of electrocoagulation process for removal of sulphate from aqueous environments using plate aluminum electrodes, World Appl. Sci. J. 7 (2009) 1526–1533.